

# The SARS-coronavirus membrane protein induces apoptosis via interfering with PDK1–PKB/Akt signalling

Ho Tsoi\*†, Li Li\*†, Zhefan S. Chen\*†, Kwok-Fai Lau†‡§, Stephen K. W. Tsui|| and Ho Yin Edwin Chan\*†‡§<sup>1</sup>

\*Laboratory of *Drosophila* Research, The Chinese University of Hong Kong, Shatin, N.T., Hong Kong, China

†Biochemistry Programme, The Chinese University of Hong Kong, Shatin, N.T., Hong Kong, China

‡Cell and Molecular Biology Programme, The Chinese University of Hong Kong, Shatin, N.T., Hong Kong, China

§Molecular Biotechnology Programme, School of Life Sciences, Faculty of Science, The Chinese University of Hong Kong, Shatin, N.T., Hong Kong, China

||School of Biomedical Sciences, Faculty of Medicine, The Chinese University of Hong Kong, Shatin, N.T., Hong Kong, China

A number of viral gene products are capable of inducing apoptosis by interfering with various cellular signalling cascades. We previously reported the pro-apoptotic property of the SARS-CoV (severe acute respiratory syndrome coronavirus) M (membrane)-protein and a down-regulation of the phosphorylation level of the cell-survival protein PKB (protein kinase B)/Akt in cells expressing M-protein. We also showed that overexpression of PDK1 (3-phosphoinositide-dependent protein kinase 1), the immediate upstream kinase of PKB/Akt, suppressed M-induced apoptosis. This illustrates that M-protein perturbs the PDK1 and PKB/Akt cell survival signalling pathway. In the present study, we demonstrated that the C-terminus of M-protein interacts with the PH (pleckstrin homology) domain of PDK1. This interaction disrupted the association between PDK1 and PKB/Akt, and led to down-regulation of PKB/Akt activity. This subsequently reduced the level of the phosphorylated forkhead transcription

factor FKHRL1 and ASK (apoptosis signal-regulating kinase), and led to the activation of caspases 8 and 9. Altogether, our data demonstrate that the SARS-CoV M-protein induces apoptosis through disrupting the interaction of PDK1 with PKB/Akt, and this causes the activation of apoptosis. Our work highlights that the SARS-CoV M protein is highly pro-apoptotic and is capable of simultaneously inducing apoptosis via initiating caspases 8 and 9. Preventing the interaction between M-protein and PDK1 is a plausible therapeutic approach to target the pro-apoptotic property of SARS-CoV.

**Key words:** apoptosis, membrane protein (M-protein), 3-phosphoinositide-dependent protein kinase-1 (PDK1), protein kinase B (PKB)/Akt, severe acute respiratory syndrome coronavirus (SARS-CoV).

## INTRODUCTION

The PKB (protein kinase B/Akt) cell survival signalling pathway has been observed to be a key in being manipulated by different viruses during the viral life cycle to achieve maximal viral production [1–5] and apoptosis [6,7]. Viral proteins can trigger viral cytopathic effect which subsequently leads to apoptosis in infected cells [6]. PKB is a serine/threonine kinase which belongs to the cAMP-dependent protein kinase A/protein kinase G/protein kinase C super family of protein kinases [8]. It is a central player in a cellular kinase cascade regulating a variety of functions, including nutrient metabolism, cell growth and cell survival [9,10]. The activity of PKB/Akt is regulated by PDK1 (3-phosphoinositide-dependent protein kinase-1), which is a serine/threonine kinase which possesses a C-terminal PH (pleckstrin homology) domain [11]. The PDK1 kinase is capable of phosphorylating a series of protein kinases, including S6K (p70 ribosomal S6 kinase) at Thr<sup>229</sup> and PKB/Akt at Thr<sup>308</sup>, for cell survival and/or proliferation [12]. The phosphorylation of S6K is mediated through protein–protein interaction between S6K and the PIF-pocket of PDK1 [13]. For PKB/Akt, PDK1 mediates PKB/Akt phosphorylation, which activates its activity, allowing it to phosphorylate its downstream substrates, including apoptosis regulatory factors such as forkhead transcription factor FKHRL1 and ASK (apoptosis signal-regulating kinase) [10].

It has also been demonstrated that PKB/Akt activity correlates with apoptosis [14]. Suppression of PKB/Akt activity has been shown to induce apoptosis [15]. The forkhead transcription factor FKHRL1 is known to regulate the expression of the potent pro-apoptotic gene *FasL* (Fas ligand) [16]. Upon phosphorylation, phospho-FKHRL1 is retained in the cytoplasm, and therefore cannot mediate the expression of *FasL*. However, once the activity of PKB/Akt is compromised, FKHRL1 translocates to the nucleus and subsequently induces *FasL* expression [17,18]. Such induction thus mediates the activation of caspase 8. In addition, suppression of PKB/Akt activity has also been reported to activate caspase 9 [19]. ASK is another substrate of PKB/Akt [20]. When the activity of PKB/Akt is suppressed, ASK is activated. Such activation subsequently phosphorylates JNK (c-Jun N-terminal kinase) and eventually leads to the activation of caspase 9 [21]. In summary, perturbation of PKB/Akt signalling leads to apoptosis via the activation of caspases.

The SARS-CoV (severe acute respiratory syndrome coronavirus) causes the highly lethal infectious disease SARS in humans [22]. The SARS-CoV genome contains 13–15 genes encoding replicases, various structural proteins, including spike, envelope, membrane, nucleocapsid and a number of accessory proteins [23–25]. Several proteins of SARS-CoV have been found to be pro-apoptotic, and the overexpression of individual viral proteins has been shown to be capable of inducing apoptosis by

Abbreviations: ASK, apoptosis signal-regulating kinase; FasL, Fas ligand; HRP, horseradish peroxidase; JNK, c-Jun N-terminal kinase; M-protein, membrane protein; PDK1, 3-phosphoinositide-dependent protein kinase 1; PH domain, pleckstrin homology domain; PKB, protein kinase B; S6K, p70 ribosomal S6 kinase; SARS-CoV, severe acute respiratory syndrome coronavirus; TUNEL, terminal deoxynucleotidyltransferase-mediated dUTP nick-end labelling.

<sup>1</sup> To whom correspondence should be addressed (email hiechan@cuhk.edu.hk).

interfering with various cell signal cascades [26–31]. Membrane (M) protein is one of the structural proteins of SARS-CoV [32,33]. M-protein mediates the incorporation of the nucleocapsid into the newly formed virions [34,35], and it recruits all of the other viral structural components to the endoplasmic reticulum–Golgi compartment for virus assembly and budding [34]. M-protein is 221 amino acids in length, it possesses a short N-terminal region (1–14), a triple membrane-spanning region (residues 15–37, 50–72 and 76–98), and a long cytosolic C-terminal domain (99–221) [32]. Our group previously reported the pro-apoptotic effect of M-protein *in vivo*. We showed that M-protein-induced apoptosis could be suppressed by both inhibitors of caspase 8 and caspase 9 [4]. In the present paper, we report that M-protein is capable of physically interacting with PDK1. Such binding disrupts the interaction between PDK1 and PKB/Akt. This reduces the level of PKB/Akt phosphorylation. As a consequence, caspase 8 and caspase 9 activation were triggered. Taken together, we have dissected the molecular mechanisms of SARS-CoV M-mediated cell death.

## EXPERIMENTAL

### Construction of mammalian expression vectors

The full-length Myc-tagged M-protein expression construct pcDNA3.1(+)-myc-Membrane1–221 has been reported previously [4]. DNA fragments encoding Myc-tagged truncated M-protein mutants were generated by PCR using pcDNA3.1(+)-myc-Membrane1–221 as a template and the following primer pairs: Membrane1–135 (MembraneF, 5'-CGGG-ATCCATGGAAGTCTCTCTGAAGAGGATCTGATGGCAG-ACAACGGTACT-3' and Membrane135R, 5'-CGCTCGAGTTAACTTTCCATGAGCGGTCT-3'); Membrane1–180 (MembraneF, 5'-CGGGATCCATGGAAGTCTCTCTGAAGAGGATCTGATGGCAGACAACGGTACT-3' and Membrane180R, 5'-CGCTCGAGTTATAATTTGTAATAAGAAAG-3'); Membrane97–221 (Membrane97F, 5'-CGGGATCCATGGAAGTCTCTCTGAAGAGGATCTGCTTCCTCAGGCTGTTT-3' and Membrane221R, 5'-CGCTCGAGTTACTGTACTAGCAAAGC-3'); Membrane97–221 (Membrane97F, 5'-CGGGATCCATGGAAGTCTCTCTGAAGAGGATCTGCTTCCTCAGGCTGTTT-3' and Membrane180R, 5'-CGCTCGAGTTATAATTTGTAATAAGAAAG-3'). The PCR fragments were cloned into BamHI and XhoI sites of pcDNA3.1(+) to generate pcDNA3.1(+)-myc-Membrane1–135, pcDNA3.1(+)-myc-Membrane1–180, pcDNA3.1(+)-myc-Membrane97–221 and pcDNA3.1(+)-myc-Membrane97–180. The constitutively active pEGFP-Akt-DD construct [36] was obtained from Addgene (plasmid 39536). A DNA fragment encoding FLAG-tagged full-length PDK1 was generated by PCR using the HKE293FT cDNA template and the following primer pairs: PDK1F, 5'-GGAATTCATGGATTACAAGGACGATGACGATAAGATGGCCAGGACCACCAGCCAGCTG-3' and PDK1R, 5'-GGCTC-TAGATCACTGCACAGCGCGTCCGGGTG-3'. The fragment was cloned into the EcoRI and XbaI sites of pcDNA3.1(+) to generate pcDNA3.1(+)-FLAG-PDK1. DNA fragments encoding PDK1 delPH and PH domain were generated by PCR using pcDNA3.1(+)-FLAG-PDK1 as template and the following primer pairs: PDK1 delPH (PDK1F and PDK1 delPHR, 5'-GGCTCTAGATCATGACCTCTGGGGCAGGCCCGTGTGTC-3'); PH domain (PHF, 5'-GGAATTCATGGATTACAAGGACGATGACGATAAGATGGACACGGCCTGCCAGAGG-3' and PDK1R). The DNA fragments were cloned into EcoRI and XbaI sites of pcDNA3.1(+) to generate pcDNA3.1(+)-FLAG-PDK1 delPH and pcDNA3.1(+)-FLAG-PH domain.

### Mammalian cell culture and transient transfection

HEK (human embryonic kidney)-293FT cells were maintained at 37°C in DMEM (Dulbecco's modified Eagle's medium; Invitrogen) supplemented with 10% FBS (Life Technologies), penicillin (100 units/ml) and streptomycin (100 g/ml). Cells were seeded on to 6- or 24-well plates 24 h prior to transfection. Plasmid DNA (2 µg for a 6-well plate or 0.4 µg for a 24-well plate) was transfected using Lipofectamine™ 2000 reagent (Life Technologies). The DNA to transfection reagent ratio was fixed at 1 µg:2 µl. Cells were harvested 48 h post-transfection.

### Immunostaining

Cells were seeded at a density of  $5 \times 10^4$  cells/well on coverslips. After 24 h, the cells were transfected with 0.5 µg of pcDNA3.1(+)-myc-Membrane1–221. Cells were fixed with 4% paraformaldehyde for 15 min at room temperature. Cells were then washed three times with PBS at room temperature each for 5 min. Cells were then permeabilized using PBS with 0.1% Triton X-100 for 15 min at room temperature. After permeabilization, cells were blocked with PBS with 5% goat serum for 30 min at room temperature. Cells were stained with anti-PDK1 (1:500 dilution; NB100-2383; Novus) and anti-Myc (1:500 dilution; 2276, Cell Signaling) antibodies in the presence of 3% BSA at 4°C overnight. Cells were washed three times with PBS, each for 5 min. Cells were then stained with FITC-conjugated anti-rabbit (1:400 dilution; 81-6111; Zymed) and Cy3 (indocarbocyanine)-conjugated anti-mouse (1:400 dilution; 81-6515; Zymed) antibodies at room temperature for 1 h. Cells were washed with PBS five times each for 5 min at room temperature. A control experiment was performed to demonstrate the specificity of the anti-PDK1 antibody. Before immunostaining, the antibody was first pre-incubated with a PDK1-blocking peptide (2 µg/ml; NB100-2383PEP; Novus) at room temperature for 30 min to deplete the anti-PDK1 antibody. Nuclei were stained with Hoechst 33342 (1:400 dilution; Life Technologies). Cells were then washed with PBS three times at room temperature. The coverslips were mounted on to glass slides with 5 µl of mounting medium (Dako). Images were captured using an Olympus FV-1000IX81-TIRF confocal microscope.

### Co-immunoprecipitation and Western blot analysis

Cells were first washed once with PBS. For 6-well plates, 200 µl of lysis buffer (20 mM Tris/HCl, pH7.4, 150 mM NaCl and 0.5% Nonidet P40) supplemented with protease inhibitor cocktail (Sigma) with a 100-fold dilution was applied to each well. The cells were sonicated using Sonifier 450 (Branson). The lysates were clarified at 16000 g for 10 min at 4°C. The supernatant was then collected and 20 µl of the sample was saved as 'input' control. For each sample, 90 µl of the supernatant was incubated either with or without antibody at 4°C overnight with shaking. The dilutions of antibodies were as follows: anti-14-3-3 (1:250 dilution; sc-1019, Santa Cruz Biotechnology), anti-PDK1 (1:200 dilution; 3062, Cell Signaling Technology), anti-Myc (1:500 dilution; 2276, Cell Signaling Technology) and anti-FLAG (1:500 dilution; F3165, Sigma). On the following day, 20 µl of Protein A-agarose fast-flow beads (Sigma) were washed twice with 1 ml of binding buffer. Lysates from the overnight incubation were incubated with washed Protein A-agarose beads at 4°C for 2 h with shaking. The Protein A-agarose beads were then washed three times with 1 ml of ice-cold binding buffer. After the final wash, the beads were resuspended in 30 µl of 6× SDS sample buffer, boiled for

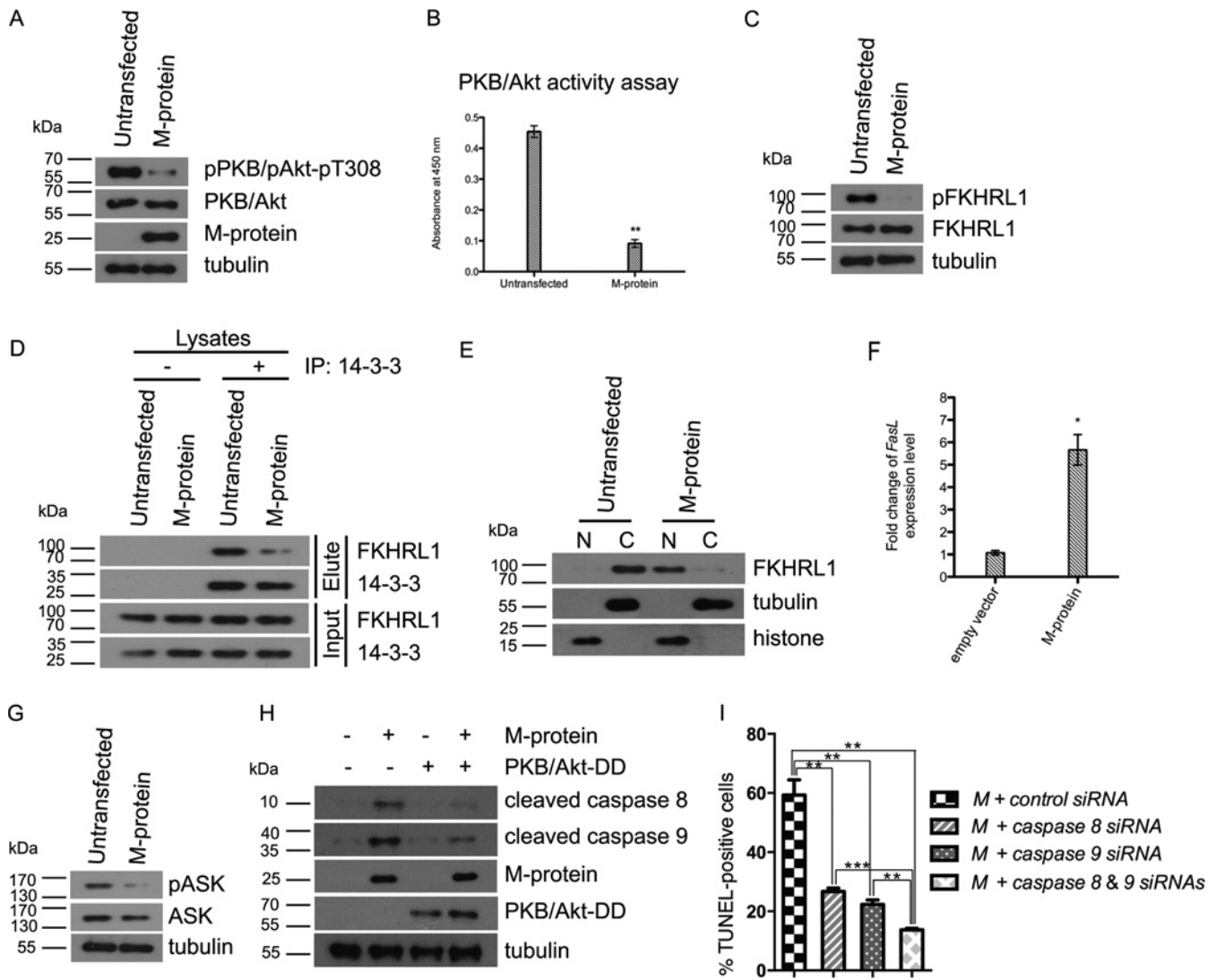


**Figure 1** M-protein of SARS-CoV induced caspase 8 and 9 activation by down-regulating the PKB/Akt signalling pathway

(A) Expression of M-protein reduced PKB/Akt phosphorylation at Thr<sup>308</sup>. The signal intensity of total PKB/Akt was similar in both untransfected and M-protein-expressing cells. Three independent experiments were performed. (B) Expression of M-protein led to suppression of PKB/Akt activity. PKB/Akt activity was determined by absorbance at 450 nm. Three independent experiments were performed. (C) M-protein compromised phosphorylation of forkhead transcription factor FKHL1. The total level of FKHL1 was not affected by M-protein expression. Three independent experiments were performed. (D) Co-immunoprecipitation (IP) of 14-3-3 with FKHL1. The presence of M-protein disrupted the association between 14-3-3 and FKHL1. + indicates that antibody was present in the immunoprecipitation reactions and – indicates that no antibody was included in the reactions. Three independent experiments were performed. (E) Nucleocytoplasmic fractionation of FKHL1. The majority of FKHL1 in untransfected cells was found in cytoplasmic fraction (C). In contrast, the majority of FKHL1 in M-protein-expressing cells was found in the nuclear fraction (N). Tubulin was used as cytoplasmic marker, whereas histone was used as nuclear marker. Three independent experiments were performed. (F) Expression of M-protein enhanced the expression level of *FasL*. Real-time PCR was employed to determine the expression level of *FasL*. The fold change of *FasL* expression level was determined with reference to untransfected cells. Three independent experiments were performed. (G) Expression of M-protein compromised the phosphorylation of ASK. The expression level of ASK was not affected by expression of M-protein. Three independent experiments were performed. (H) Expression of constitutively active PKB/Akt (PKB/Akt-DD) suppressed the activation of caspases 8 and 9 in M-protein-expressing cells. Tubulin was used as a loading control. Only representative blots are shown. (I) Knockdown of caspase 8 and caspase 9 expression blocked SARS-CoV M-protein-mediated caspase 8- and 9-dependent apoptosis. Apoptosis was detected using the APO-BrdU<sup>TM</sup> TUNEL Assay kit, with Alexa Fluor<sup>®</sup> 488 Anti-BrdU<sup>TM</sup> (Life Technologies). The histograms show means  $\pm$  S.D. from three independent experiments. At least 100 cells were counted in each experiment. \* $P < 0.05$ , \*\* $P < 0.01$  and \*\*\* $P < 0.001$ . Molecular masses are indicated in kDa.

10 min and followed by Western blot analysis as described previously [37]. Primary antibodies used were anti-Akt (1:1000 dilution; 9272, Cell Signaling Technology), anti-pAkt (1:1000 dilution; 4056; Cell Signaling Technology), anti-PDK1 (1:500 dilution; 5662; Cell Signaling Technology), anti-FKHRL1 (1:200 dilution; sc-11351; Santa Cruz Biotechnology), anti-pFKHRL1 (1:500 dilution; sc-12357, Santa Cruz Biotechnology), anti-14-3-3 (1:400 dilution; sc-1019, Santa Cruz Biotechnology), anti-ASK (1:1000 dilution; 3762; Cell Signaling Technology), anti-pASK

(1:1000 dilution; 3761, Cell Signaling Technology), anti-Myc (1:2000 dilution, 2276 or 2278; Cell Signaling Technology), anti-FLAG (1:4000 dilution; M2; Sigma or 1:2000 dilution; 8146; Cell Signaling Technology), anti-cleaved caspase 8 (1:100 dilution; 9748; Cell Signaling Technology), anti-cleaved caspase 9 (1:100 dilution; 9501; Cell Signaling Technology); anti-S6K (1:200 dilution; 2708P; Cell Signaling Technology); anti-pS6K (1:100 dilution; SAB4503955; Sigma); anti-caspase 8 (1:500 dilution; ab11919; Abcam); anti-caspase 9 (1:1000 dilution; 9502; Cell Signaling Technology); anti-tubulin (1:10000 dilution;

E7; Developmental Studies Hybridoma Bank) and anti-histone (1:5000 dilution; ab47915; Abcam). Secondary antibodies used were HRP (horseradish peroxidase)-conjugated goat anti-mouse IgG (1:2000 dilution; 7076; Cell Signaling Technology), HRP-conjugated goat anti-rabbit IgG (1:2000 dilution; 7074; Cell Signaling Technology) and HRP-conjugated rabbit anti-goat IgG (1:2000 dilution; R-21459, Life Technologies).

### PKB/Akt activity assay

PKB/Akt activity assay was measured using a K-LISA™ Akt Activity Kit (Calbiochem) according to the manufacturer's instructions. EnVision® Multilabel Reader (PerkinElmer) was used for signal detection. Each experiment was performed in triplicate and repeated at least three times.

### Real-time PCR

Total RNA was extracted from cells using TRIzol® reagent (Life Technologies) and 0.5 µg of total RNA was reverse transcribed using the ImPromII® Reverse Transcription System (Promega). Taqman gene expression assays were performed on an ABI 7500 Real-time PCR system using following probes: *FasL* (Hs00181225\_m1; Life Technologies) and *actin* (Hs99999903\_m1; Life Technologies). Each experiment was performed in triplicate and was repeated at least three times. Quantification of gene expression was calculated according to the  $2^{-\Delta\Delta C_T}$  method [38].

### Nucleocytoplasmic fractionation

Cytoplasmic and nuclear protein fractions were prepared as described previously [39]. In brief, cells were homogenized in fractionation buffer (10 mM Tris/HCl, pH 7.4, 10 mM NaCl, 3 mM MgCl<sub>2</sub> and 0.5% Nonidet P40). The cell lysates were centrifuged at 16000 g. The supernatant was collected as the cytoplasmic fraction. The pellet was extracted using resuspension buffer (10 mM Tris/HCl, pH 7.4, 10 mM NaCl, 3 mM MgCl<sub>2</sub>, 0.5% Nonidet P40 and 2% SDS) and then collected as the nuclear fraction.

### TUNEL (terminal deoxynucleotidyltransferase-mediated dUTP nick-end labelling) assay

The TUNEL assay was performed according to [40]. In brief, cells were seeded at  $7 \times 10^5$  on to 6-cm-diameter dishes. After 24 h, cells were transfected with 35 nM caspase 8 siRNA or 10 nM caspase 9 siRNA for 48 h, followed by transfection with pcDNA3.1(+)-myc-Membrane 1-221 construct for 48 h. Apoptosis was measured using the APO-BrdU™ TUNEL assay kit with Alexa Fluor® 488 anti-BrdU (Life Technologies) according to the manufacturer's instructions.

### Statistical analyses

Statistical analyses were performed using two-tailed unpaired Student's *t* test. All experiments were performed at least three times. Results are presented as means ± S.D. A *P* value of less than 0.05 was considered to be statistically significant.

## RESULTS

### SARS-CoV M-protein activated caspase cascades by modulating the activities of Forkhead transcription factor FKHRL1 and ASK

We previously reported that expression of SARS-CoV M-protein caused a down-regulation of PKB/Akt phosphorylation in a *Drosophila* model [4]. Consistent with our previous result, we detected a reduced phosphorylated PKB/Akt level (Figure 1A) and diminished PKB/Akt activity (Figure 1B) in mammalian cells expressing M-protein. One of the functions of PKB/Akt is to regulate forkhead transcription factor FKHRL1 for cell survival [18]. Phosphorylation of FKHRL1 is essential for interacting with 14-3-3 protein [18]. When such protein-protein interaction is abolished, FKHRL1 translocates to the nucleus where it mediates pro-apoptotic gene expression [18]. Since we observed a down-regulation of PKB/Akt activity in M-protein-expressing cells, we decided to investigate the phosphorylation status of FKHRL1 and found that the level of phosphorylated FKHRL1 was reduced (Figure 1C). By means of co-immunoprecipitation, we also found that the interaction between FKHRL1 and 14-3-3 was diminished in M-protein-expressing cells (Figure 1D). We next investigated the subcellular localization of FKHRL1 in the presence of M-protein. In untransfected cells, majority of FKHRL1 was detected in the cytoplasmic fraction (Figure 1E). In contrast, FKHRL1 was enriched in the nuclear fraction when M-protein was expressed (Figure 1E). *FasL* is a pro-apoptotic gene whose expression is regulated by FKHRL1 [41]. By means of real-time PCR, we showed that the expression level of *FasL* was elevated significantly in M-protein-expressing cells (Figure 1F). Consistent with the well-established role of *FasL* in caspase 8 activation [41], we also observed caspase 8 cleavage in M-protein-expressing cells (Figure 1H). Therefore our results reveal that the expression of M-protein causes activation of caspase 8.

Our previous study demonstrated that treatment of either the caspase 8 inhibitor Z-IETD-FMK (benzyloxycarbonyl-Ile-Glu-Thr-DL-Asp-fluoromethylketone) or the caspase 9 inhibitor Z-LEHD-FMK (benzyloxycarbonyl-Leu-Glu-His-DL-Asp-fluoromethylketone), only partially suppressed M-protein-induced apoptosis [4]. This suggests that both caspases 8 and 9 are involved in M-protein-induced apoptosis. ASK is a substrate of PKB/Akt [20] and a down-regulation of ASK phosphorylation leads to caspase 9 activation [42]. Therefore, we investigated the phosphorylation status of ASK in M-protein-expressing cells. We observed a reduction in the level of phosphorylated ASK (Figure 1G). Furthermore, we detected caspase 9 cleavage (Figure 1H) in these cells. When we co-expressed M-protein with a constitutively active form of PKB/Akt [36], cleavage of caspases 8 and 9 was suppressed (Figure 1H). Taken together, our results demonstrated that expression of M-protein causes activation of both caspases 8 and 9 via the PKB/Akt signalling cascades. To confirm further our findings, we knocked down the expression of caspase 8 and caspase 9 individually and together (Supplementary Figure S1) to determine the effect of these knockdowns on M-induced apoptosis using the TUNEL assay. We found that both caspases 8 and 9 are involved in M-protein-induced cell death, and the simultaneous knockdown of caspases 8 and 9 caused a more significant cell death blockade (Figure 1I).

### The C-terminus of M-protein interacts with the PH domain of PDK1

The expression of SARS-CoV M-protein has previously been reported to trigger cell death [43]. Given that we observed a down-regulation of PKB/Akt-pThr<sup>308</sup> phosphorylation level

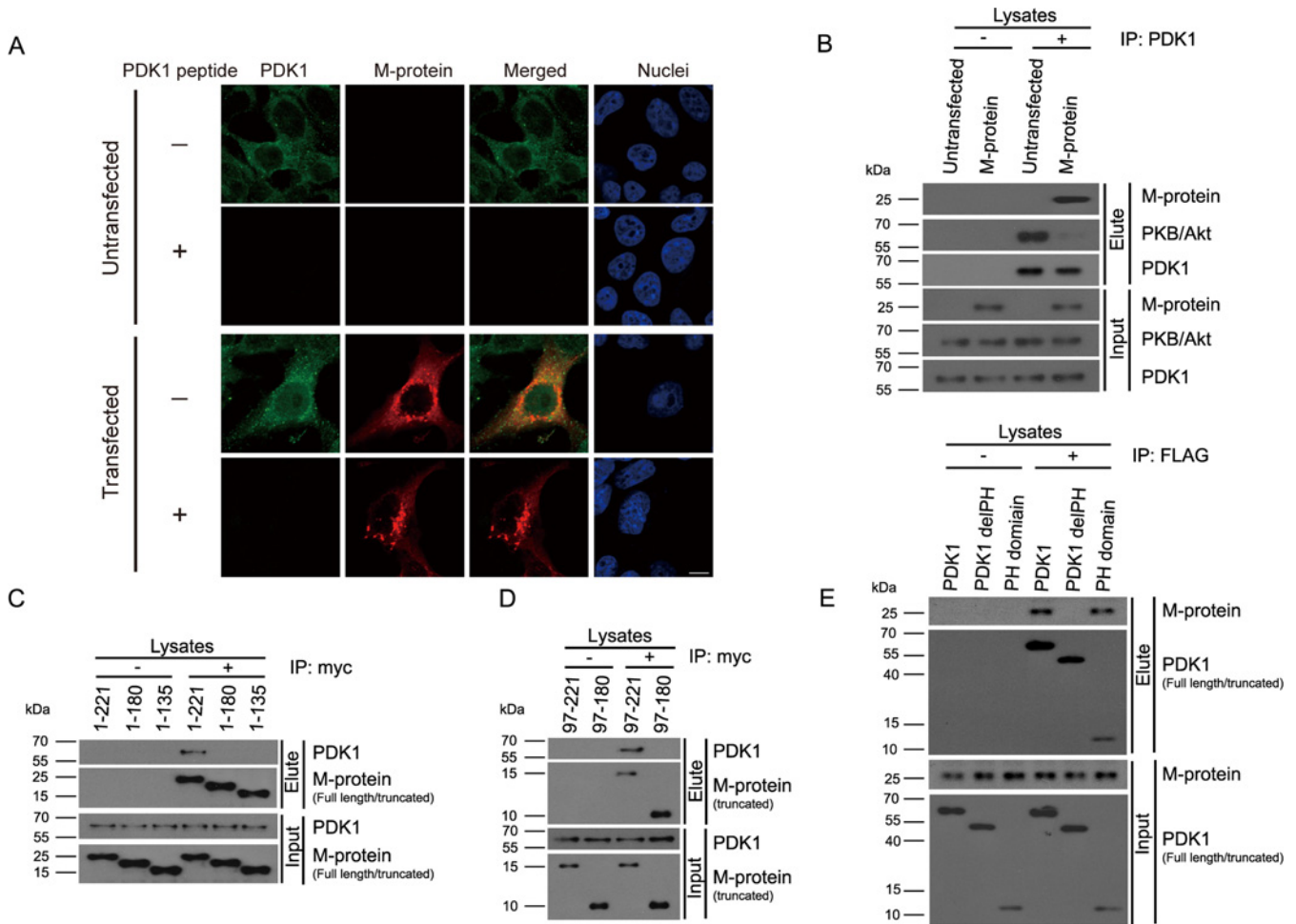


**Figure 2** M-protein competes with PKB/Akt for PDK1

(A) Co-localization of M-protein and PDK1. M-protein (red) was stained with anti-Myc antibody and endogenous PDK1 (green) was stained with anti-PDK1 antibody. Untransfected and transfected represent cells without and with M-protein expression respectively; +, anti-PDK1 antibody was depleted by PDK1 peptide; -, no PDK1 peptide was added to deplete anti-PDK1. Cell nuclei (in blue) were stained with Hoechst 33342. Scale bar, 10  $\mu$ m. At least three independent experiments were performed. (B) Co-immunoprecipitation of PDK1 with PKB/Akt. In untransfected cells, PKB/Akt was able to associate with PDK1. However, in M-protein-expressing cells, M-protein was found to bind to PDK1, and the association between PKB/Akt and PDK1 was disrupted. Three independent experiments were performed. (C) The C-terminus of M-protein was responsible for interacting with PDK1. Co-immunoprecipitation was performed. Only full-length (1-221) M-protein was able to interact with PDK1, but not the other two truncated M-proteins (1-180 and 1-135). Three independent experiments were performed. (D) The N-terminus of M-protein was dispensable for PDK1 interaction. Truncated M-protein (97-221) was able to interact with PDK1, but not another truncated M-protein (97-180). Three independent experiments were performed. (E) The PH domain of PDK1 was responsible for interacting with M-protein. Co-immunoprecipitation was performed. Full-length PDK1 was able to interact with M-protein, but the deletion mutant PDK1 delPH was not able to interact with M-protein. The PH domain of PDK1 alone was sufficient to interact with M-protein. +, antibody was present in the immunoprecipitation reactions; -, no antibody was included in the reactions. Three independent experiments were performed. Only representative blots are shown. Molecular masses in kDa are indicated. IP, immunoprecipitation.

in M-protein expressing cells [4] (Figure 1A), and that we identified PDK1, an immediate upstream kinase of PKB/Akt, as a genetic suppressor of M-protein-induced apoptosis *in vivo* [4], we investigated the underlying mechanism through which caspases 8 and 9 are activated in M-protein-expressing cells (Figure 1). PKB is a substrate of PDK1 [11], and down-regulation of PDK1 reduces the level of phosphorylated PKB/Akt and caspase activation [44]. We hypothesized that M-protein disrupts the interaction between PDK1 and PKB/Akt, which then leads to reduction of PKB/Akt phosphorylation. By means of confocal microscopy, we detected co-localization of M-protein and PDK1 in the cytosol (Figure 2A). We next determined whether M-protein interacted biochemically with PDK1. To do this, we first showed that PKB/Akt interacted with PDK1 in untransfected cells in serum-containing culture medium (Figure 2B and Supplementary Figure S2); and such interaction was diminished in cells expressing M-protein. Concomitantly, PDK1 was found to associate with M-

protein (Figure 2B). The results thus indicate that the PDK1-M-protein and PDK1-PKB/Akt interactions are mutually exclusive.

To identify the region of M-protein responsible for interacting with PDK1, four M-protein deletion mutants (1-180, 1-135, 97-180 and 97-221) were generated. Co-immunoprecipitation results showed that all M-protein deletion mutants (including 1-180), except for 97-221, failed to interact with PDK1 (Figures 2C and 2D). Taken together, our data indicate that M-protein employs its C-terminal domain (181-221) to interact with PDK1. We showed further that the expression of an M-protein fragment (97-221) was capable of disrupting the interaction between PDK1 and PKB/Akt (Figure 2B and Supplementary Figure S3). This highlights the functional significance of the C-terminal domain of M-protein in perturbing cell survival signalling. Since PDK1 interacts with PKB/Akt via its PH domain, we investigated whether M-protein would bind to the PH domain of PDK1. To test this, we generated a PDK1 deletion mutant construct (PDK1

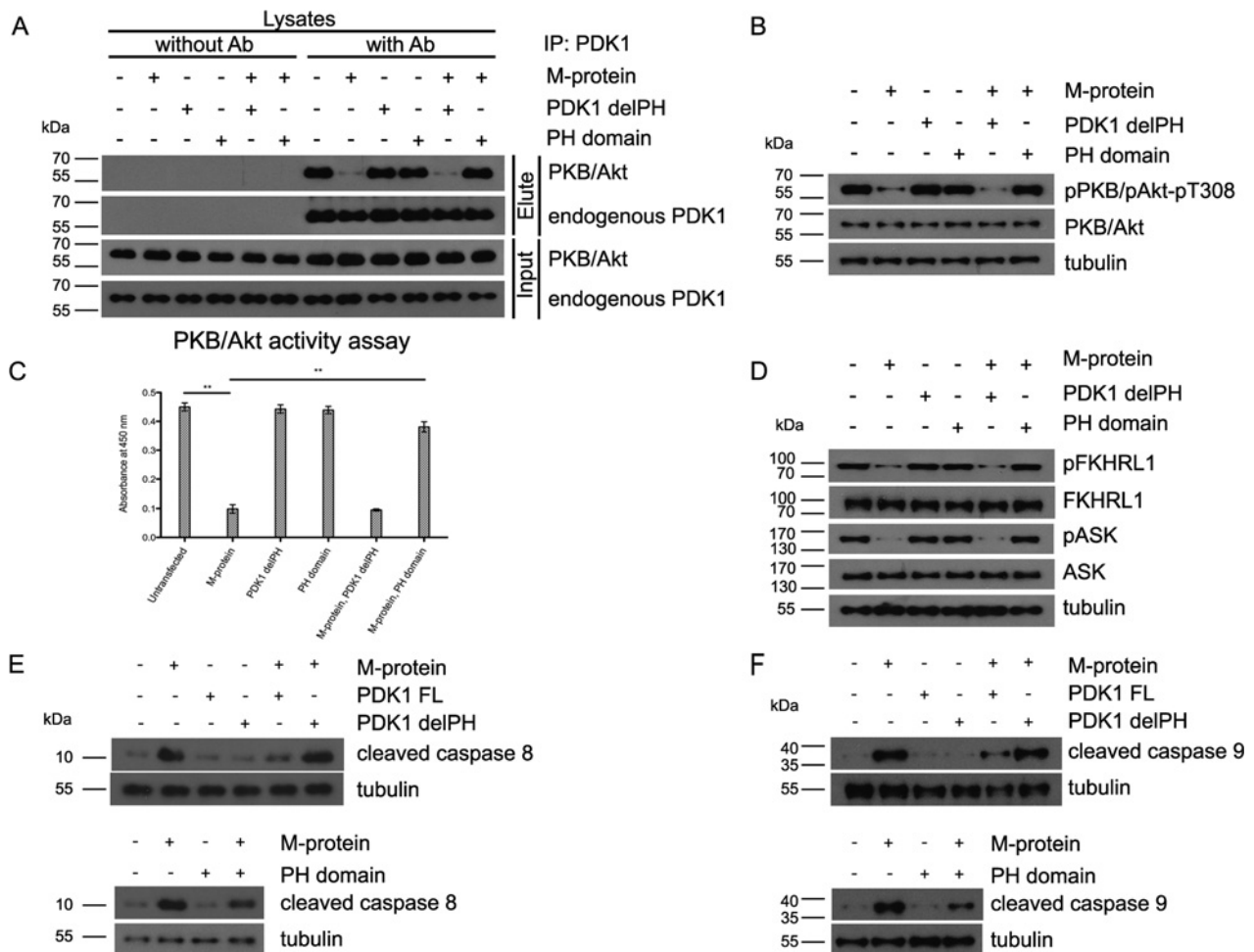


**Figure 3** Expression of PDK1 PH domain restored the PDK1–PKB/Akt-mediated signalling cascade

(A) Expression of PDK1 PH domain restored the interaction between PDK1 and PKB/Akt in M-protein-expressing cells. Three independent experiments were performed. Co-expression of PDK1 PH domain restored the phosphorylation of PKB/Akt at Thr<sup>308</sup> (B), activity of PKB/Akt (C), and the phosphorylation of FKHRL1 and ASK (D) in M-protein-expressing cells. Three independent experiments were performed. Expression of PDK1 PH domain suppressed the cleavage of caspase 8 (E) and caspase 9 (F) induced by M-protein. Tubulin was used as a loading control. Results in (C) are means  $\pm$  S.D. \*\* $P < 0.01$ . Only representative blots are shown, with molecular masses in kDa. Ab, antibody; IP, immunoprecipitation.

delPH) which lacks the PH domain, and another construct, PDK1 PH domain, which only carries the PH domain of PDK1. We found that PDK1 delPH did not interact with M-protein (Figure 2E). This indicates that the PH domain is essential for mediating the PDK1–M-protein interaction. Consistent with this view, we found that the PDK1 PH domain itself was capable of interacting with M-protein (Figure 2E). We also showed that M-protein did not alter S6K (another PDK1 substrate) phosphorylation (Supplementary Figure S4). The interaction between S6K and PDK1 is mediated through the PIF-pocket of PDK1 [45], and our finding suggests M-protein preferentially perturbs the activity of any PDK1 downstream substrate whose phosphorylation is mediated through its PH domain. In summary, our findings provide an explanation of how M-protein competes with PKB/Akt for interacting with PDK1.

To investigate further whether the diminished PKB/Akt activity we observed in M-protein-expressing cells (Figure 1B) was solely caused by the binding of M-protein to endogenous PDK1, we examined whether interfering with the M-protein–PDK1 interaction would restore endogenous PDK1–PKB/Akt interaction. To test this, we co-expressed M-protein with either the PDK1 delPH or PDK1 PH domain, and determined endogenous

PDK1–PKB/Akt interaction. We found that the co-expression of PDK1 PH domain largely restored endogenous PDK1–PKB/Akt association (Figure 3A and Supplementary Figure S5), whereas PDK1 delPH failed to do so. This is consistent with our above result that PDK1 delPH was unable to bind to M-protein (Figure 2E). We showed further that co-expression of the PDK1 PH domain restored PKB/Akt phosphorylation (Figure 3B), PKB/Akt activity (Figure 3C), phosphorylation of FKHRL1 and ASK (Figure 3D), and subsequently suppressed the activation and cleavage of caspase 8 (Figure 3E) and caspase 9 (Figure 3F) in M-protein-expressing cells. Our results thus indicate that the down-regulation of PDK1–PKB/Akt activity is a key event in M-protein-induced apoptosis.

## DISCUSSION

Viral proteins have long been associated with apoptosis. For example, apoptin of the chicken anaemia virus, gp120 and gp41 of HIV-1, HPV (human papillomavirus)-18 of papillomaviruses and NS1 of the influenza virus have been reported to induce apoptosis [46]. In the present study, we elucidated the molecular

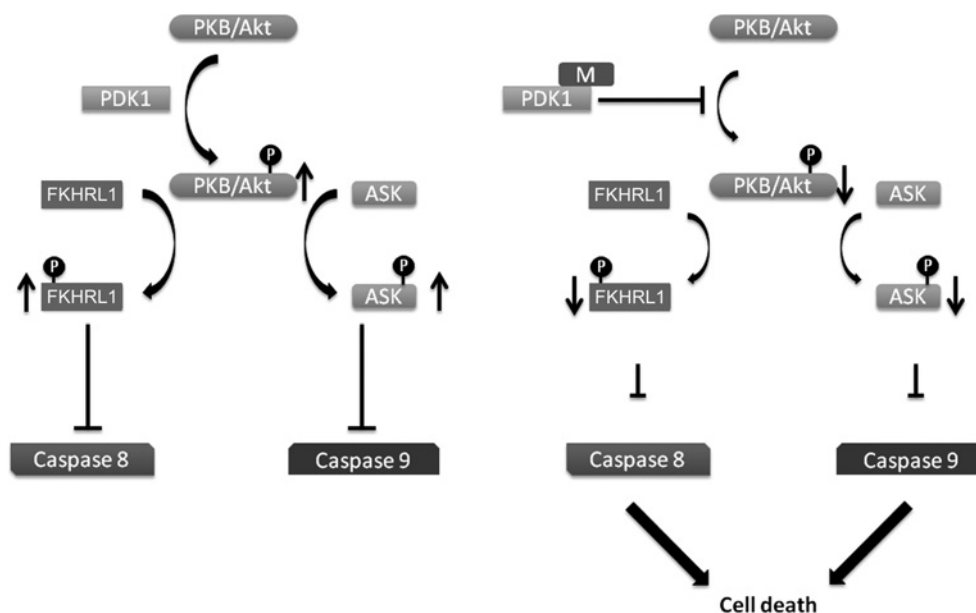


**Figure 4** Proposed model for SARS-CoV signalling

M-protein mediates caspase 8- and 9-dependent apoptosis. PDK1 mediates the phosphorylation of PKB/Akt which in turn regulates the phosphorylation status of FKHL1 and ASK. Phosphorylation of FKHL1 and ASK inhibits the activation of caspase 8 and caspase 9. SARS-CoV M-protein binds to PDK1, and this interaction compromises the phosphorylation of PKB/Akt. Subsequently, the level of phosphorylated FKHL1 and ASK is down-regulated. Caspase 8 and caspase 9 activities are no longer inhibited and apoptosis is triggered.

mechanism that the SARS-CoV M-protein exploits to induce cell death. The M-protein compromises PKB/Akt activity by interfering with its upstream activator PDK1. This in turn upsets the balance of phosphorylation status of downstream PKB/Akt targets. Such an alteration of phosphorylation balance of cellular proteins causes downstream cellular physiological consequences, including apoptosis [9,10]. In the present study, we showed that M-protein expression caused a down-regulation of FKHL1 phosphorylation (Figure 1C). This subsequently led to an enrichment of FKHL1 in the nuclear compartment (Figure 1E). FKHL1 is a transcription factor that governs the expression level of *FasL* [16]. Once the level of *FasL* is increased, this eventually leads to the activation of caspase 8 [41]. Our previous findings indicate that the blockade of caspase 8 or caspase 9 activity only partially inhibits cell death [4]. This indicates that caspase 8 is probably not the only mediator of cell death induced by M-protein. ASK is a substrate of PKB/Akt [47], and it has been reported that PKB/Akt regulates ASK activity [20]. When PKB/Akt activity is down-regulated, ASK activity is derepressed, which causes JNK activation [20]. Subsequently, phosphorylated JNK leads to cell death through the activation of caspase 9 [21]. As PKB/Akt activity was compromised by M-protein, down-regulation of ASK phosphorylation was observed in M-expressing cells (Figure 1G) followed by caspase 9 cleavage (Figure 1H). Our finding is consistent with previous investigations that down-regulation of PKB/Akt activity was observed in SARS-CoV-infected cells [2,3]. The present study shows that M-protein is one of the culprits leading to PKB/Akt down-regulation in SARS-CoV infection, and this in turn compromises cell survival signalling which eventually triggers apoptosis (Figure 4).

We have demonstrated that M-protein induces caspase 8 and caspase 9 activation by down-regulating the PKB/Akt survival signalling cascade. We found that the C-terminus of M-protein (residues 97–221) is responsible for interacting with the PH domain of PDK1 (Figure 2). Such an interaction compromised the

interaction between PKB/Akt and PDK1. Since PDK1 mediates PKB/Akt phosphorylation, blocking the access of PKB/Akt to PDK1 prevents PKB/Akt activation. Subsequently, the PKB/Akt signalling cascade is compromised. To confirm further that this interaction is essential for M-protein to induce cell death, we investigated whether the co-expression of the PH domain of PDK1 could counteract M-mediated apoptosis. The rationale behind this was to introduce a binding partner of M-protein; therefore the exogenous PH domain could bind to M-protein, allowing the endogenous PDK1 to interact with PKB/Akt. Our results demonstrated that the co-expression of PH domain and M-protein could restore the interaction between PDK1 and PKB/Akt (Figure 3A). Our results also showed that expression of the PDK1 PH domain itself showed no modulatory effect on PKB/Akt activity (Figure 3). We thus anticipate that the rescuing effect of the PDK1 PH domain is probably mediated through its interaction with the M-protein, which indicates specificity towards the M-protein. In summary, our investigations show that the SARS-CoV M-protein is capable of interacting with PDK1, through which it compromises cellular pro-survival signalling and subsequently activates caspase cascades. The present study provides new evidence for the participation of two parallel pro-apoptotic pathways in SARS-CoV M-protein-induced cell death. The results shown in the present paper will broaden our understanding of the pro-apoptotic role of M-protein. Identifying inhibitors that have high affinity towards the C-terminal direction to counteract SARS-CoV M-protein-mediated cell death.

#### AUTHOR CONTRIBUTION

Ho Tsoi, Kwok-Fai Lau, Stephen Kwok-Wing Tsui and Ho Yin Edwin Chan designed the study. Ho Tsoi, Li Li and Zhefan S Chen carried out the experiments and analysed the data. All of the authors discussed the results, Ho Tsoi and Ho Yin Edwin Chan wrote the paper.

## FUNDING

This work was supported by the Hong Kong Food and Health Bureau Research Fund for the Control of Infectious Diseases [grant number 08070492], Research Grants Council of Hong Kong [grant number AoE/M-05/12] and the Chinese University of Hong Kong (CUHK) Research Fellowship Scheme [grant number 4200348].

## ACKNOWLEDGEMENTS

We thank Shirley Chan for technical support and members of the Laboratory of *Drosophila* Research for critical reading of the paper before submission.

## REFERENCES

- Mizutani, T., Fukushi, S., Saijo, M., Kurane, I. and Morikawa, S. (2004) Phosphorylation of p38 MAPK and its downstream targets in SARS coronavirus-infected cells. *Biochem. Biophys. Res. Commun.* **319**, 1228–1234 [CrossRef PubMed](#)
- Mizutani, T., Fukushi, S., Saijo, M., Kurane, I. and Morikawa, S. (2004) Importance of Akt signaling pathway for apoptosis in SARS-CoV-infected Vero E6 cells. *Virology* **327**, 169–174 [CrossRef PubMed](#)
- Mizutani, T., Fukushi, S., Saijo, M., Kurane, I. and Morikawa, S. (2005) JNK and PI3K/Akt signaling pathways are required for establishing persistent SARS-CoV infection in Vero E6 cells. *Biochim. Biophys. Acta* **1741**, 4–10 [CrossRef PubMed](#)
- Chan, C. M., Ma, C. W., Chan, W. Y. and Chan, H. Y. E. (2007) The SARS-coronavirus membrane protein induces apoptosis through modulating the Akt survival pathway. *Arch. Biochem. Biophys.* **459**, 197–207 [CrossRef PubMed](#)
- Soares, J. A. P., Leite, F. G. G., Andrade, L. G., Torres, A. A., De Sousa, L. P., Barcelos, L. S., Teixeira, M. M., Ferreira, P. C. P., Kroon, E. G., Souto-Padron, T. and Bonjardim, C. A. (2009) Activation of the PI3K/Akt pathway early during vaccinia and cowpox virus infections is required for both host survival and viral replication. *J. Virol.* **83**, 6883–6899 [CrossRef PubMed](#)
- Yan, H. M., Xiao, G. F., Zhang, J. M., Hu, Y. Y., Yuan, F., Cole, D. K., Zheng, C. G. and Gao, G. F. (2004) SARS coronavirus induces apoptosis in Vero E6 cells. *J. Med. Virol.* **73**, 323–331 [CrossRef PubMed](#)
- Ren, L. L., Yang, R. Q., Guo, L., Qu, J. G., Wang, J. W. and Hung, T. (2005) Apoptosis induced by the SARS-associated coronavirus in Vero cells is replication-dependent and involves caspase. *DNA Cell Biol.* **24**, 496–502 [CrossRef PubMed](#)
- Song, G., Ouyang, G. L. and Bao, S. D. (2005) The activation of Akt/PKB signaling pathway and cell survival. *J. Cell. Mol. Med.* **9**, 59–71 [CrossRef PubMed](#)
- Manning, B. D. and Cantley, L. C. (2007) AKT/PKB signaling: navigating downstream. *Cell* **129**, 1261–1274 [CrossRef PubMed](#)
- Liao, Y. and Hung, M. C. (2010) Physiological regulation of Akt activity and stability. *Am. J. Transl. Res.* **2**, 19–42 [PubMed](#)
- Mora, A., Komander, D., van Aalten, D. M. F. and Alessi, D. R. (2004) PDK1, the master regulator of AGC kinase signal transduction. *Semin. Cell Dev. Biol.* **15**, 161–170 [CrossRef PubMed](#)
- Alessi, D. R., James, S. R., Downes, C. P., Holmes, A. B., Gaffney, P. R., Reese, C. B. and Cohen, P. (1997) Characterization of a 3-phosphoinositide-dependent protein kinase which phosphorylates and activates protein kinase B $\alpha$ . *Curr. Biol.* **7**, 261–269 [CrossRef PubMed](#)
- Najafov, A., Shpiro, N. and Alessi, D. R. (2012) Akt is efficiently activated by PIF-pocket- and PtdIns(3,4,5)P<sub>3</sub>-dependent mechanisms leading to resistance to PDK1 inhibitors. *Biochem. J.* **448**, 285–295 [CrossRef PubMed](#)
- Franke, T. F., Hornik, C. P., Segev, L., Shostak, G. A. and Sugimoto, C. (2003) PI3K/Akt and apoptosis: size matters. *Oncogene* **22**, 8983–8998 [CrossRef PubMed](#)
- Datta, S. R., Brunet, A. and Greenberg, M. E. (1999) Cellular survival: a play in three Akts. *Gene Dev.* **13**, 2905–2927 [CrossRef](#)
- Kavurma, M. M. and Khachigian, L. M. (2003) Signaling and transcriptional control of Fas ligand gene expression. *Cell Death Differ.* **10**, 36–44 [CrossRef PubMed](#)
- Suhara, T., Kim, H. S., Kirshenbaum, L. A. and Walsh, K. (2002) Suppression of Akt signaling induces Fas ligand expression: involvement of caspase and jun kinase activation in Akt-mediated Fas ligand regulation. *Mol. Cell. Biol.* **22**, 680–691 [CrossRef PubMed](#)
- Brunet, A., Bonni, A., Zigmond, M. J., Lin, M. Z., Juo, P., Hu, L. S., Anderson, M. J., Arden, K. C., Blenis, J. and Greenberg, M. E. (1999) Akt promotes cell survival by phosphorylating and inhibiting a Forkhead transcription factor. *Cell* **96**, 857–868 [CrossRef PubMed](#)
- Lawlor, M. A. and Alessi, D. R. (2001) PKB/Akt: a key mediator of cell proliferation, survival and insulin responses? *J. Cell Sci.* **114**, 2903–2910 [PubMed](#)
- Kim, A. H., Khursigara, G., Sun, X., Franke, T. F. and Chao, M. V. (2001) Akt phosphorylates and negatively regulates apoptosis signal-regulating kinase 1. *Mol. Cell Biol.* **21**, 893–901 [CrossRef PubMed](#)
- Dhanasekaran, D. N. and Reddy, E. P. (2008) JNK signaling in apoptosis. *Oncogene* **27**, 6245–6251 [CrossRef PubMed](#)
- Cheng, V. C. C., Lau, S. K. P., Woo, P. C. Y. and Yuen, K. Y. (2007) Severe acute respiratory syndrome coronavirus as an agent of emerging and reemerging infection. *Clin. Microbiol. Rev.* **20**, 660–694 [CrossRef PubMed](#)
- Marra, M. A., Jones, S. J. M., Astell, C. R., Holt, R. A., Brooks-Wilson, A., Butterfield, Y. S. N., Khattra, J., Asano, J. K., Barber, S. A., Chan, S. Y. et al. (2003) The genome sequence of the SARS-associated coronavirus. *Science* **300**, 1399–1404 [CrossRef PubMed](#)
- Rota, P. A., Oberste, M. S., Monroe, S. S., Nix, W. A., Campagnoli, R., Icenogle, J. P., Penaranda, S., Bankamp, B., Maher, K., Chen, M. H. et al. (2003) Characterization of a novel coronavirus associated with severe acute respiratory syndrome. *Science* **300**, 1394–1399 [CrossRef PubMed](#)
- Ksiazek, T. G., Erdman, D., Goldsmith, C. S., Zaki, S. R., Peret, T., Emery, S., Tong, S. X., Urbani, C., Comer, J. A., Lim, W. et al. (2003) A novel coronavirus associated with severe acute respiratory syndrome. *New Engl. J. Med.* **348**, 1953–1966 [CrossRef](#)
- Surjit, M., Liu, B. P., Jameel, S., Chow, V. T. K. and Lal, S. K. (2004) The SARS coronavirus nucleocapsid protein induces actin reorganization and apoptosis in COS-1 cells in the absence of growth factors. *Biochem. J.* **383**, 13–18 [CrossRef PubMed](#)
- Wong, S. L. A., Chen, Y. W., Chan, C. M., Chan, C. S. M., Chan, P. K. S., Chui, Y. L., Fung, K. P., Wayne, M. M. Y., Tsui, S. K. W. and Chan, H. Y. E. (2005) *In vivo* functional characterization of the SARS-coronavirus 3a protein in *Drosophila*. *Biochem. Biophys. Res. Commun.* **337**, 720–729 [CrossRef PubMed](#)
- Mizutani, T., Fukushi, S., Saijo, M., Kurane, I. and Morikawa, S. (2004) Phosphorylation of p38 MAPK and its downstream targets in SARS coronavirus-infected cells. *Biochem. Biophys. Res. Commun.* **319**, 1228–1234 [CrossRef PubMed](#)
- Lin, C. W., Lin, K. H., Hsieh, T. H., Shiu, S. Y. and Li, J. Y. (2006) Severe acute respiratory syndrome coronavirus 3C-like protease-induced apoptosis. *FEMS Immunol. Med. Microbiol.* **46**, 375–380 [CrossRef PubMed](#)
- Chow, K. Y. C., Yeung, Y. S., Hon, C. C., Zeng, F. Y., Law, K. M. and Leung, F. C. C. (2005) Adenovirus-mediated expression of the C-terminal domain of SARS-CoV spike protein is sufficient to induce apoptosis in Vero E6 cells. *FEBS Lett.* **579**, 6699–6704 [CrossRef PubMed](#)
- Chan, C. M., Tsoi, H., Chan, W. M., Zhai, S., Wong, C. O., Yao, X., Chan, W. Y., Tsui, S. K. and Chan, H. Y. (2009) The ion channel activity of the SARS-coronavirus 3a protein is linked to its pro-apoptotic function. *Int. J. Biochem. Cell Biol.* **41**, 2232–2239 [CrossRef PubMed](#)
- Voss, D., Pfefferle, S., Drosten, C., Stevermann, L., Tragglia, E., Lanzavecchia, A. and Becker, S. (2009) Studies on membrane topology, N-glycosylation and functionality of SARS-CoV membrane protein. *Virology* **493**, 6 [CrossRef](#)
- He, Y. X., Zhou, Y. S., Siddiqui, P., Niu, J. K. and Jiang, S. B. (2005) Identification of immunodominant epitopes on the membrane protein of the severe acute respiratory syndrome-associated coronavirus. *J. Clin. Microbiol.* **43**, 3718–3726 [CrossRef PubMed](#)
- Siu, Y. L., Teoh, K. T., Lo, J., Chan, C. M., Kien, F., Escrivou, N., Tsao, S. W., Nicholls, J. M., Altmeyer, R., Peiris, J. S. M. et al. (2008) The M, E, and N structural proteins of the severe acute respiratory syndrome coronavirus are required for efficient assembly, trafficking, and release of virus-like particles. *J. Virol.* **82**, 11318–11330 [CrossRef PubMed](#)
- Hatakeyama, S., Matsuoka, Y., Ueshiba, H., Komatsu, N., Itoh, K., Shichijo, S., Kanai, T., Fukushi, M., Ishida, I., Kirikae, T. et al. (2008) Dissection and identification of regions required to form pseudoparticles by the interaction between the nucleocapsid (N) and membrane (M) proteins of SARS coronavirus. *Virology* **380**, 99–108 [CrossRef PubMed](#)
- Watton, S. J. and Downward, J. (1999) Akt/PKB localisation and 3' phosphoinositide generation at sites of epithelial cell-matrix and cell-cell interaction. *Curr. Biol.* **9**, 433–436 [CrossRef PubMed](#)
- Tsoi, H., Lau, T. C. K., Tsang, S. Y., Lau, K. F. and Chan, H. Y. E. (2012) CAG expansion induces nucleolar stress in polyglutamine diseases. *Proc. Natl. Acad. Sci. U.S.A.* **109**, 13428–13433 [CrossRef PubMed](#)
- Livak, K. J. and Schmittgen, T. D. (2001) Analysis of relative gene expression data using real-time quantitative PCR and the 2<sup>- $\Delta\Delta$ CT</sup> method. *Methods* **25**, 402–408 [CrossRef PubMed](#)
- Chan, W. M., Tsoi, H., Wu, C. C., Wong, C. H., Cheng, T. C., Li, H. Y., Lau, K. F., Shaw, P. C., Perrimon, N. and Chan, H. Y. E. (2011) Expanded polyglutamine domain possesses nuclear export activity which modulates subcellular localization and toxicity of polyQ disease protein via exportin-1. *Hum. Mol. Genet.* **20**, 1738–1750 [CrossRef PubMed](#)
- Tsoi, H., Yu, A. C., Chen, Z. S., Ng, N. K., Chan, A. Y., Yuen, L. Y., Abrigo, J. M., Tsang, S. Y., Tsui, S. K., Tong, T. M. et al. (2014) A novel missense mutation in CCDC88C activates the JNK pathway and causes a dominant form of spinocerebellar ataxia. *J. Med. Genet.* **51**, 590–595 [CrossRef PubMed](#)
- Nagata, S. (1999) Fas ligand-induced apoptosis. *Annu. Rev. Genet.* **33**, 29–55 [CrossRef PubMed](#)

- 42 Takeda, K., Matsuzawa, A., Nishitoh, H. and Ichijo, H. (2003) Roles of MAPKKK ASK1 in stress-induced cell death. *Cell Struct. Funct.* **28**, 23–29 [CrossRef PubMed](#)
- 43 Lai, C. W., Chan, Z. R., Yang, D. G., Lo, W. H., Lai, Y. K., Chang, M. D. T. and Hu, Y. C. (2006) Accelerated induction of apoptosis in insect cells by baculovirus-expressed SARS-CoV membrane protein. *FEBS Lett.* **580**, 3829–3834 [CrossRef PubMed](#)
- 44 Nakajima, H., Sakaguchi, K., Fujiwara, I., Mizuta, M., Tsuruga, M., Magae, J. and Mizuta, N. (2007) Apoptosis and inactivation of the PI3-kinase pathway by tetrocarcin A in breast cancers. *Biochem. Biophys. Res. Commun.* **356**, 260–265 [CrossRef PubMed](#)
- 45 Biondi, R. M., Kieloch, A., Currie, R. A., Deak, M. and Alessi, D. R. (2001) The PIF-binding pocket in PDK1 is essential for activation of S6K and SGK, but not PKB. *EMBO J.* **20**, 4380–4390 [CrossRef PubMed](#)
- 46 O'Brien, V. (1998) Viruses and apoptosis. *J. Gen. Virol.* **79**, 1833–1845 [PubMed](#)
- 47 Ichijo, H., Nishida, E., Irie, K., tenDijke, P., Saitoh, M., Moriguchi, T., Takagi, M., Matsumoto, K., Miyazono, K. and Gotoh, Y. (1997) Induction of apoptosis by ASK1, a mammalian MAPKKK that activates SAPK/JNK and p38 signaling pathways. *Science* **275**, 90–94 [CrossRef PubMed](#)

---

Received 4 November 2013/22 September 2014; accepted 1 October 2014  
Published as BJ Immediate Publication 1 October 2014, doi:10.1042/BJ20131461